

Enhancing Laser Ablation ICP-MS Using Sector Field Technology

Key Words

- ELEMENT 2
- Geochronology
- Isotope Ratios
- Laser Ablation
- Multi-Element Analysis

Introduction

Laser ablation inductively coupled plasma-mass spectrometry (LA-ICP-MS) has developed over recent years to become a sophisticated tool for the multi-elemental and isotope ratio analysis of solid samples. Besides a true multi-elemental capability, independent of matrix, the major requirements for most geological laser applications in ICP-MS are the highest sensitivity and scan speed. Such demanding analytical pre-requisites often require the most sophisticated instrumentation, such as the Thermo Scientific ELEMENT 2.

This Application Report describes a variety of LA-ICP-MS applications from different scientists to provide a brief summary of the technique in their particular fields of interest. The contributions included are:

- Pb geochronology in zircons (M. Tiepolo et al.)
- Re and Os concentration measurements in molybdenite (I. Rodushkin et al.)
- High mass resolution for non-matrix dependent laser ablation analysis, the isotopic analysis of Pleistocene human remains and the multi-element analysis of fluid inclusions by LA-ICP-MS, (Ch. Latkoczy et al.)

In Situ Pb Geochronology of Zircons

Massimo Tiepolo

Email: tiepolo@crystal.unipv.it

web: http://www_crystal.unipv.it

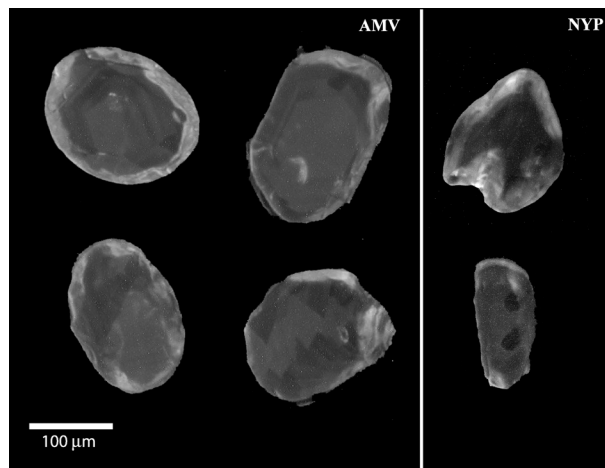


Figure 1: Typical zircons analyzed in this study.

The Pb geochronological capabilities of sector field LA-ICP-MS, based on the coupling of the Thermo Scientific ELEMENT and a 213 nm UV laser, have been tested on a series of zircons (Figure 1) ranging in age between 150 and 577 Ma (Figure 2):

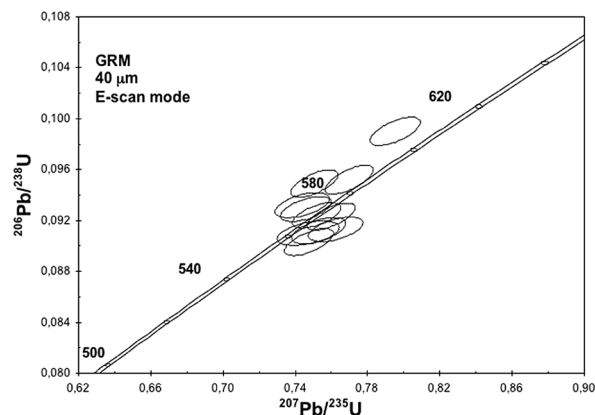


Figure 2: Geochronological determination of zircons.

- Geologically meaningful ages calculated from the ratios $^{206}\text{Pb}/^{238}\text{U}$, $^{207}\text{Pb}/^{235}\text{U}$ and $^{208}\text{Pb}/^{232}\text{Th}$ can be achieved down to 1 ppm of total Pb in zircon. Reliable $^{207}\text{Pb}/^{206}\text{Pb}$ ages can be only achieved in zircons with $> \sim 40$ ppm of total Pb.
- At a spatial resolution of 40 μm , the electrostatic scan mode (EScan) is more suitable and gives internal precision values on $^{206}\text{Pb}/^{238}\text{U}$, $^{207}\text{Pb}/^{235}\text{U}$ and $^{208}\text{Pb}/^{232}\text{Th}$ ages to better than 1.1% (for zircons with ~ 40 ppm of total Pb).
- A spatial resolution of 20 μm can be used on relatively Pb-rich zircons even if the internal precision is about 1.5 times lower than with a spot size of 40 μm .
- Accuracy is not particularly sensitive to scan mode and is more influenced by the total Pb content of zircon, with values ranging between 1 and 5%.

Reference

Tiepolo M., In situ Pb geochronology of zircon with laser ablation-inductively coupled plasma-sector field mass spectrometry. *Chemical Geology*, 2003, 199, 159-177.

Determination of Re and Os Concentrations in Molybdenite

Ilia Rodushkin

Email: ilia.rodushkin@analytica.se

web: <http://www.analytica.se>



Figure 3: Thermo Scientific ELEMENT 2 with New Wave UP213 laser system.

The ^{187}Re - ^{187}Os geochronometer applied to molybdenite has been demonstrated to be remarkably robust, surviving intense rock deformation and high-grade thermal metamorphism. In molybdenite virtually all Os is produced by the radioactive decay of ^{187}Re to ^{187}Os . Successful dating by isotope dilution techniques is dependent on careful preparation of the mineral separate and on the appropriate choice of spikes. Both the Re and Os contents of molybdenites are highly variable, requiring pre-information for the preparation of the correct spike amounts. LA-ICP-MS (Figure 3) is therefore used as a rapid tool for Re and Os determination in molybdenite, since sample preparation for LA-ICP-MS consists of only the separation of the molybdenite, followed by grinding and pressing to form pellets.

External calibration with internal standardization using a matrix-matched standard has been found to be the best quantification approach for Re, providing results that are indistinguishable from data obtained by solution based ID-ICP-MS (within the limits of measurement precision). The accuracy of ^{187}Os quantification by LA-ICP-MS is poorer than compared to Re, as its determination requires the correction of a severe isobaric interference from ^{187}Re . Consequently, the determination only gives results that are more accurate for the older and higher in Os molybdenite samples.

References

Malinovsky D., Rodushkin I., Axelsson M.D., and D.C. Baxter, Determination of rhenium and osmium concentrations in molybdenite using laser ablation double focusing sector field ICP-MS. *Journal of Geochemical Exploration*, 2004, 81, 71-79.

Malinovsky D., Rodushkin I., Baxter D. and B. Öhlander, Simplified method for the Re-Os dating of molybdenite using acid digestion and isotope dilution ICP-MS. *Analytica Chimica Acta*, 2002, 463, 111-124.

Multi-Element Trace Analysis of Synthetic Mineral Materials

Christopher Latkoczy, Magne Ødegard and Detlef Günther

Email: Latkoczy@inorg.chem.ethz.ch

web: <http://www.analytica.ethz.ch>

The quantification of trace elements in synthetically prepared mineral standards used for microanalysis (rutile TiO_2 , apatite $\text{Ca}_3(\text{PO}_4)_2$ and fluorite CaF_2) by LA-ICP-MS coupled to a 193 nm ArF - Excimer laser system was investigated. A commercially available standard silicate reference material (NIST SRM 612) was used as a one point calibration standard. Using such a non-matrix matched calibration procedure, a highly linear correlation between the measured and nominal concentrations for elements doped to the material was established (Figure 4).

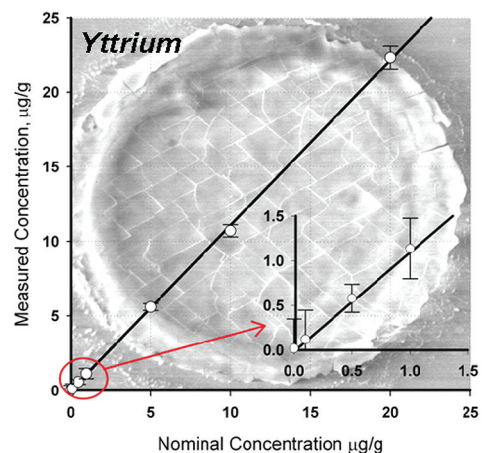


Figure 4: Typical 193 nm ArF - Excimer laser crater in CaF_2 . Calibration curve using NIST SRM 612 as external standard.

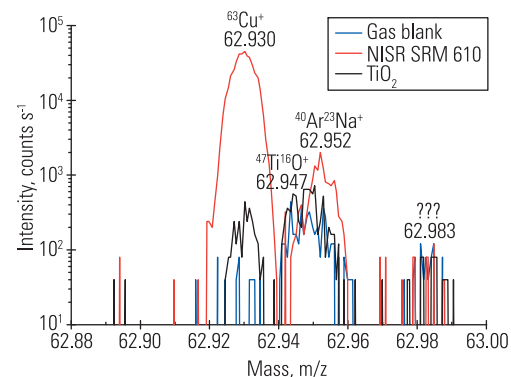


Figure 5a: Medium resolution ($R = 4000$) spectrum at m/z 63 separating ^{63}Cu from the main interferences.

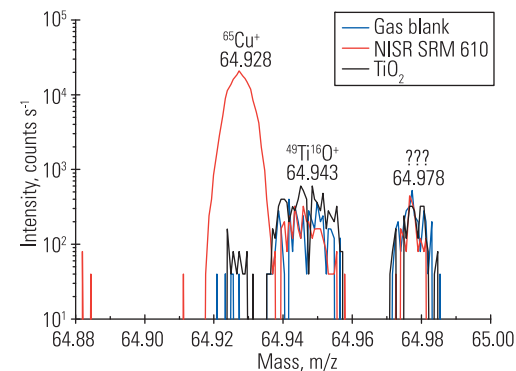


Figure 5b: Medium resolution ($R = 4000$) spectrum at m/z 65 separating ^{65}Cu from the main interferences.

Furthermore, the enhanced mass resolution capabilities of the instrument was used to identify possible interferences resulting from major sample elements (Figure 5a and 5b). The materials were analyzed using different laser spot sizes, ranging from 10 - 120 μm in order to study the elemental distribution of the elements in the mineral standards. At a spot size of 60 μm , relative standard deviations (RSDs) for 10 consecutive measurements were below 5% for the apatite, below 11% for the fluorite, and below 18% for the rutile (Figure 6). The accuracy for each element in the three synthetic mineral standards was within 15% for most elements in the apatite and fluorite materials, and up to 23% in the rutile. Such LA-ICP-MS studies proved to be very useful in order to characterize the homogeneity of synthetically prepared materials in the micrometer-scale.

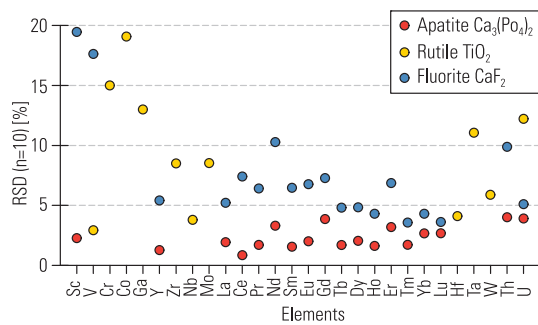


Figure 6: Heterogeneity (expressed as % RSD for ten consecutive measurements) of various elements in the three sample materials.

References

Ødegard, M.; Skar, O.; Schiellerup, H.; Pearson, N. J., Preparation of a synthetic titanite glass calibration material for in situ microanalysis by direct fusion in graphite electrodes: A preliminary characterisation by EPMA and LA-ICP-MS, *Geostandards and Geoanalytical Research*, 2005, 29(2), 197-209.

Trace Element and Sr Isotopic Ratio Analysis of Pleistocene Human Teeth from the Altai Massif, Russia

Christopher Latkoczy, Bence Viola, Maria Teschler-Nicola, Horst Seidler, Thomas Prohaska, Beat Aeschlimann and Detlef Günther

Email: Latkoczy@inorg.chem.ethz.ch

web: <http://www.analytica.ethz.ch>

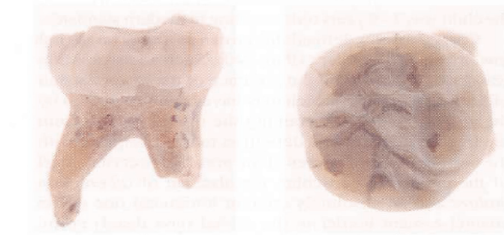


Figure 7a: Second lower right milk molar from Okladnikov cave. Left side: vestibular norm, right side: vertical norm.

In the 1980s, human remains (seven teeth and postcranial fragments) were discovered in two caves in north-western Altai, Siberia. Morphologically and metrically, the Denisova and Okladnikov cave teeth have been compared to both Neanderthals and modern humans (Figures 7a and 7b).

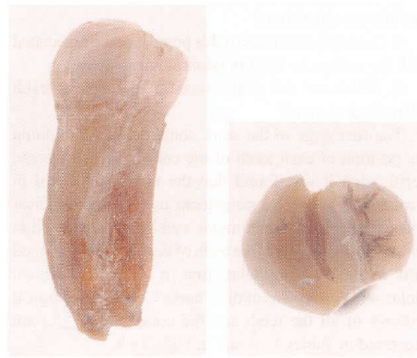


Figure 7b: First lower left premolar from Okladnikov cave. Left side: distal norm. Right side: vertical norm.

In this study, we applied LA-ICP-MS to perform a multielement analysis to assess the probability of individual association for these human remains (Figure 8).

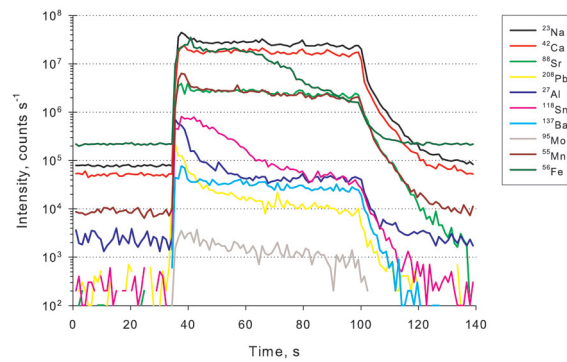


Figure 8: Multielemental laser analysis trace.

Furthermore, we used an optimized fast-scan method to measure the isotope ratio of $^{87}\text{Sr}/^{86}\text{Sr}$ in dentine and enamel to study possible migration patterns (Figure 9 and Table 1).

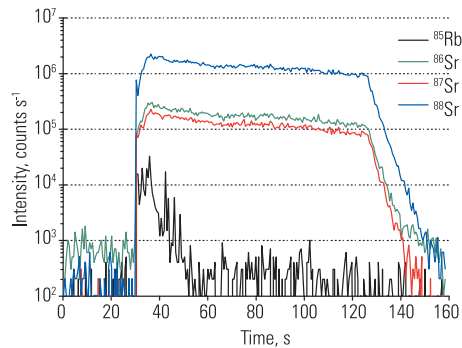


Figure 9: Strontium isotopic laser analysis trace.

	$^{87}\text{Sr} / ^{86}\text{Sr}$		
Enamel	0.711	0.711	avg
		0.001	std
		0.15%	rsd
		0.712	
Dentine		0.712	
	0.710	0.711	avg
		0.001	std
		0.09%	rsd
		0.711	
	0.710		

Table 1: Results from the Sr isotopic analysis.

Our preliminary results showed that further work is necessary to assess the amount and pattern of intra-individual variations in multi-element and isotopic composition, as well any possible effect from the post-depositional environment. We could not reach fully conclusive results on individual associations, but our results do not support previous claims that the Okladnikov cave teeth originate from only two individuals. Strontium isotope ratios in the Okladnikov sample indicate within the measurement uncertainty that the individual did not migrate, at least not to regions with strongly different geological substrate. Further information on regional geology and isotopic composition will help to clarify this question.

References

Shpakova, E.G., Derevianko, A.P., The interpretation of odontological features of Pleistocene Human Remains from the Altai, *Archaeology, Ethnology and Anthropology of Eurasia*, 2000, 1, 125-138.

Analysis of Fluid Inclusions Using Sector Field LA-ICP-MS

Christopher Latkoczy and Detlef Günther

Email: Latkoczy@inorg.chem.ethz.ch

web: <http://www.analytica.ethz.ch>

Microscopic fluid inclusions in minerals are the main source of information about the chemical composition of fluids associated with large-scale material transport in the Earth's interior. Hydrothermal transport processes are responsible for the natural enrichment of metal resources in many ore deposits. For the multi-element analysis of the microscopic fluid inclusions (typically 5 - 50 μm in diameter), LA-ICP-MS has become one of the most promising techniques owing to the recent progress in laser optics design and the development of high-sensitivity, fast-scanning ICP mass spectrometers.

Isotope	Acquire Mass	Method	Mass Offset	Mass Window	Mass Range	Magnet Mass	Setting Time	Sample Time	Sample Per Peak	Segment Duration	Search Window	Integration Window	Scan Type	Detection Mode	Integration Type
Li7	7.0155	-0.0021	20	7.013 - 7.018	7.011	0.100	0.0020	50	0.020	100	100	100	EScan	Both	Average
B11	11.0098	-0.0000	20	11.009 - 11.012	11.009	0.216	0.0020	50	0.020	100	100	100	EScan	Both	Average
Mu23	22.9092	0.0023	20	22.912 - 22.917	22.909	0.230	0.0020	50	0.020	100	100	100	EScan	Both	Average
Ma25	24.9852	0.0034	20	24.977 - 24.994	22.969	0.001	0.0020	50	0.020	100	100	100	EScan	Both	Average
N13	13.0033	0.0180	20	13.000 - 13.006	13.003	0.026	0.0020	50	0.020	100	100	100	EScan	Both	Average
Na23	22.9892	0.0044	20	22.985 - 22.993	22.989	0.001	0.0020	50	0.020	100	100	100	EScan	Both	Average
Al27	26.9815	0.0044	20	26.977 - 26.985	26.981	0.001	0.0020	50	0.020	100	100	100	EScan	Both	Average
S32	31.9720	0.0044	20	31.968 - 31.972	31.972	0.001	0.0020	50	0.020	100	100	100	EScan	Both	Average
Cl35	34.9688	0.0044	20	34.964 - 34.968	34.968	0.001	0.0020	50	0.020	100	100	100	EScan	Both	Average
Ar39	38.9637	0.0044	20	38.959 - 38.963	38.963	0.001	0.0020	50	0.020	100	100	100	EScan	Both	Average
K39	38.9637	0.0044	20	38.959 - 38.963	38.963	0.001	0.0020	50	0.020	100	100	100	EScan	Both	Average
Ca40	39.9624	0.0044	20	39.958 - 39.962	39.962	0.001	0.0020	50	0.020	100	100	100	EScan	Both	Average
Sc45	44.9559	0.0044	20	44.952 - 44.956	44.956	0.001	0.0020	50	0.020	100	100	100	EScan	Both	Average
Ti48	47.9471	0.0044	20	47.943 - 47.947	47.947	0.001	0.0020	50	0.020	100	100	100	EScan	Both	Average
V51	50.9439	0.0044	20	50.940 - 50.944	50.944	0.001	0.0020	50	0.020	100	100	100	EScan	Both	Average
Cr52	51.9405	0.0044	20	51.937 - 51.941	51.941	0.001	0.0020	50	0.020	100	100	100	EScan	Both	Average
Mn55	54.9380	0.0044	20	54.934 - 54.938	54.938	0.001	0.0020	50	0.020	100	100	100	EScan	Both	Average
Fe56	55.9349	0.0044	20	55.931 - 55.935	55.935	0.001	0.0020	50	0.020	100	100	100	EScan	Both	Average
Ni58	57.9353	0.0044	20	57.932 - 57.936	57.936	0.001	0.0020	50	0.020	100	100	100	EScan	Both	Average
Cu63	62.9296	0.0044	20	62.926 - 62.930	62.930	0.001	0.0020	50	0.020	100	100	100	EScan	Both	Average
Zn66	65.9260	0.0044	20	65.923 - 65.927	65.927	0.001	0.0020	50	0.020	100	100	100	EScan	Both	Average
As75	74.9216	0.0044	20	74.918 - 74.922	74.922	0.001	0.0020	50	0.020	100	100	100	EScan	Both	Average
Se78	77.9233	0.0044	20	77.920 - 77.924	77.924	0.001	0.0020	50	0.020	100	100	100	EScan	Both	Average
Br81	80.9163	0.0044	20	80.913 - 80.917	80.917	0.001	0.0020	50	0.020	100	100	100	EScan	Both	Average
Kr84	83.9128	0.0044	20	83.910 - 83.914	83.914	0.001	0.0020	50	0.020	100	100	100	EScan	Both	Average
Rb85	85.4678	0.0044	20	85.465 - 85.469	85.469	0.001	0.0020	50	0.020	100	100	100	EScan	Both	Average
Sr86	86.9088	0.0044	20	86.906 - 86.910	86.910	0.001	0.0020	50	0.020	100	100	100	EScan	Both	Average
Y89	88.9058	0.0044	20	88.904 - 88.906	88.906	0.001	0.0020	50	0.020	100	100	100	EScan	Both	Average
Zr90	90.9050	0.0044	20	90.903 - 90.907	90.907	0.001	0.0020	50	0.020	100	100	100	EScan	Both	Average
Nb93	92.9063	0.0044	20	92.905 - 92.907	92.907	0.001	0.0020	50	0.020	100	100	100	EScan	Both	Average
Mo96	95.9046	0.0044	20	95.903 - 95.905	95.905	0.001	0.0020	50	0.020	100	100	100	EScan	Both	Average
Ru101	100.9055	0.0044	20	100.904 - 100.906	100.906	0.001	0.0020	50	0.020	100	100	100	EScan	Both	Average
Rh103	102.9055	0.0044	20	102.904 - 102.906	102.906	0.001	0.0020	50	0.020	100	100	100	EScan	Both	Average
Pd106	105.9063	0.0044	20	105.905 - 105.907	105.907	0.001	0.0020	50	0.020	100	100	100	EScan	Both	Average
Ag107	106.9056	0.0044	20	106.904 - 106.906	106.906	0.001	0.0020	50	0.020	100	100	100	EScan	Both	Average
Cd111	110.9041	0.0044	20	110.903 - 110.905	110.905	0.001	0.0020	50	0.020	100	100	100	EScan	Both	Average
In113	112.9044	0.0044	20	112.903 - 112.905	112.905	0.001	0.0020	50	0.020	100	100	100	EScan	Both	Average
Sn115	114.9043	0.0044	20	114.903 - 114.905	114.905	0.001	0.0020	50	0.020	100	100	100	EScan	Both	Average
Sb115	114.9043	0.0044	20	114.903 - 114.905	114.905	0.001	0.0020	50	0.020	100	100	100	EScan	Both	Average
Te128	127.9056	0.0044	20	127.904 - 127.906	127.906	0.001	0.0020	50	0.020	100	100	100	EScan	Both	Average
I127	126.9054	0.0044	20	126.904 - 126.906	126.906	0.001	0.0020	50	0.020	100	100	100	EScan	Both	Average
Xe131	130.9051	0.0044	20	130.904 - 130.906	130.906	0.001	0.0020	50	0.020	100	100	100	EScan	Both	Average
Ba137	136.9053	0.0086	20	136.900 - 136.910	136.905	0.001	0.0020	50	0.020	100	100	100	EScan	Both	Average
La139	138.9048	0.0122	20	138.886 - 138.922	138.908	0.021	0.0020	50	0.020	100	100	100	EScan	Both	Average
Ce140	139.9049	0.0186	20	139.888 - 139.922	139.908	0.001	0.0020	50	0.020	100	100	100	EScan	Both	Average
Pr141	140.9047	0.0186	20	140.887 - 140.900	140.900	0.024	0.0020	50	0.020	100	100	100	EScan	Both	Average
Nd142	141.9046	0.0186	20	141.886 - 141.900	141.900	0.024	0.0020	50	0.020	100	100	100	EScan	Both	Average
Sm147	146.9045	0.0255	20	146.880 - 146.910	146.900	0.001	0.0020	50	0.020	100	100	100	EScan	Both	Average
Eu151	150.9048	0.0345	20	150.870 - 150.930	150.900	0.001	0.0020	50	0.020	100	100	100	EScan	Both	Average
Gd152	151.9048	0.0345	20	151.870 - 151.930	151.900	0.001	0.0020	50	0.020	100	100	100	EScan	Both	Average
Tb157	158.9048	0.0473	20	158.860 - 158.950	158.905	0.001	0.0020	50	0.020	100	100	100	EScan	Both	Average
Dy163	162.9048	0.0641	20	162.850 - 162.950	162.900	0.001	0.0020	50	0.020	100	100	100	EScan	Both	Average
Ho165	164.9048	0.0641	20	164.850 - 164.950	164.900	0.001	0.0020	50	0.020	100	100	100	EScan	Both	Average
Er167	167.9048	0.0641	20	167.850 - 167.950	167.900	0.001	0.0020	50	0.020	100	100	100	EScan	Both	Average
Tm169	168.9048	0.0641	20	168.850 - 168.950	168.900	0.001	0.0020	50	0.020	100	100	100	EScan	Both	Average
Yb171	170.9048	0.0641	20	170.850 - 170.950	170.900	0.001	0.0020	50	0.020	100	100	100	EScan	Both	Average
Lu175	174.9048	0.0854	20	174.850 - 174.950	174.900	0.001	0.0020	50	0.020	100	100	100	EScan	Both	Average

Figure 9: ELEMENT Method file used for the analysis of fluid inclusions.

Legal Notices

©2006, 2016 Thermo Fisher Scientific Inc. All rights reserved. All trademarks are the property of Thermo Fisher Scientific Inc. and its subsidiaries. This information is presented as an example of the capabilities of Thermo Fisher Scientific Inc. products. It is not intended to encourage use of these products in any manners that might infringe the intellectual property rights of others. Specifications, terms and pricing are subject to change. Not all products are available in all countries. Please consult your local sales representative for details.

The latest improvement in the Thermo Scientific ELEMENT 2 scan speed allows magnetic jumps from the lowest mass analyzed, ^7Li , to the highest mass, ^{238}U , in only 90 ms. The jump back to the lowest mass is performed in < 50 ms.

The method developed for the analyses of 28 major, minor and trace elements, covering a concentration range of five orders of magnitude, results in a scan duration of 0.88 s and a duty cycle of 63% (Figure 9).

These analyses were carried out on single natural fluid inclusions (Figure 10) together with a number of experiments to optimize a controlled ablation technique and to test a calibration procedure.

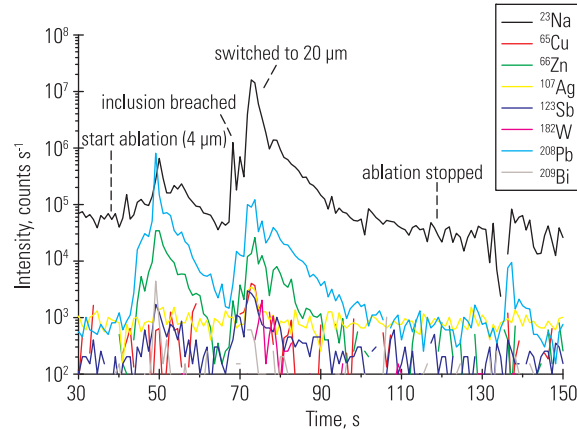


Figure 10: Time resolved laser ablation analysis of a natural fluid inclusion.

The optimized setup for sector field LA-ICP-MS was used together with a laser ablation system based on a 193 nm ArF - Excimer laser. In a procedure to stepwise open complex multiphase inclusions, a small hole (4 μm diameter) was first drilled for the partial release of liquid and vapor, followed by complete drilling out, using a laser spot size covering the entire inclusion.

References

Latkoczy, Ch., and Günther, D., Enhanced sensitivity in inductively coupled plasma sector field mass spectrometry for direct solid analysis using laser ablation (LA-ICP-SF-MS), *Journal of Analytical Atomic Spectrometry*, 2002, 17, 1264-1270.

Acknowledgements

Thermo Fisher Scientific wants to thank all authors for their contribution.

In addition to these offices, Thermo Fisher Scientific maintains a network of representative organizations throughout the world.

Australia
+61 2 8844 9500
Austria
+43 1 333 50340
Belgium
+32 2 482 30 30
Canada
+1 800 532 4752
China
+86 10 5850 3588
Denmark
+45 70 23 62 60
France
+33 1 60 92 48 00
Germany
+49 6103 408 1014
India
+91 22 6742 9434
Italy
+39 02 950 591
Japan
+81 45 453 9100
Latin America
+1 808 276 5659
Netherlands
+31 76 587 98 88
South Africa
+27 11 570 1840
Spain
+34 91 657 4930
Sweden/Norway/Finland
+46 8 556 468 00
Switzerland
+41 61 48784 00
UK
+44 1442 233555
USA
+1 800 532 4752

www.thermo.com

AN30101_E 08/16C